

# *Recovering Flapping Frequency in a Separated Flow*

S. Cherubini<sup>1,2</sup> J.-Ch. Robinet<sup>2</sup> P. De Palma<sup>1</sup>

<sup>1</sup>Politecnico di Bari, Italy

<sup>2</sup>Arts et Métiers ParisTech, France

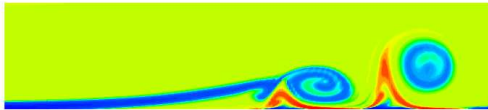
October 13, 2008

# Outline

- 1 Motivations
- 2 Numerical tools
  - Direct Numerical Simulation
  - Global model
- 3 Linear dynamics
  - Asymptotic dynamics
  - Optimal growth dynamics
- 4 Flapping frequency
  - Flapping frequency in a linear regime
  - Flapping frequency in a non-linear regime
  - Physical interpretation and scaling law
- 5 Conclusions

# Motivations

## The destabilization of a separated flow



- The primary instability of a flat plate separated flow is characterized by a three-dimensional steady and weakly growing eigenmode.
- On the other hand, laminar separation bubbles show a high sensitivity to external noise and a strong two-dimensional instability mechanism known as “flapping”.
- We would investigate in a linear and non-linear framework:
  - 1 the role of the convective modes with respect to the flapping phenomenon;
  - 2 the mechanism of transition from convective to global instability;
  - 3 the influence of topological flow changes on the stability behaviour.

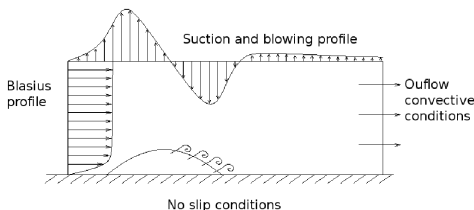
# Direct Numerical Simulation

2D non-dimensional incompressible Navier-Stokes equations

$$\begin{aligned} \mathbf{u}_t + (\mathbf{u} \cdot \nabla) \mathbf{u} &= -\nabla p + \frac{1}{Re} \nabla^2 \mathbf{u}, \\ \nabla \cdot \mathbf{u} &= 0, \end{aligned} \quad (1)$$

where  $\mathbf{u} = (u, v)^T$  is the velocity vector,  $p$  is the pressure and  $Re = \frac{U_\infty \delta^*}{\nu}$

- *Fractional step* method on a *staggered* grid.
- Spatial discretization: centered second order for the linear terms, compact sixth order for the non-linear terms (Chu & Fan 1999).
- Temporal discretization: Crank–Nicholson for the viscous terms, third-order low-storage Runge-Kutta for the non-linear terms.



# Global model

The instantaneous variables  $\mathbf{q} = (u, v, p)^T$  are considered as a superposition of the base flow and of the perturbation  $\tilde{\mathbf{q}} = (\tilde{u}, \tilde{v}, \tilde{p})^T$ .

Decomposition of the perturbations in a temporal modes basis

$$\tilde{\mathbf{q}}(x, y, t) = \sum_{k=1}^{N_t} \kappa_k^0 \hat{\mathbf{q}}_k(x, y) \exp(-i\omega_k t), \quad (2)$$

where  $N_t$  is the number of modes,  $\hat{\mathbf{q}}_k$  are the eigenvectors,  $\omega_k$  are the complex eigenmodes, and  $\kappa_k^0$  is the initial amplitude of each mode.

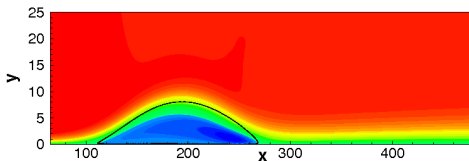
*Substituting in the NS equations and a linearizing lead to the following eigenvalue problem*

$$(\mathbf{A} - i\omega_k \mathbf{B}) \hat{\mathbf{q}}_k = \mathbf{0}, \quad k = 1, \dots, N_t. \quad (3)$$

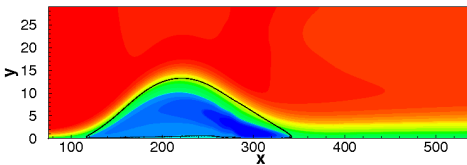
*which is discretized with a Chebyshev/Chebyshev spectral method employing  $N_t = 850$  modes on a  $270 \times 50$  grid, and it is solved with a shift and invert Arnoldi algorithm using the ARPACK library.*

# Base flow computation

$Re = 200$



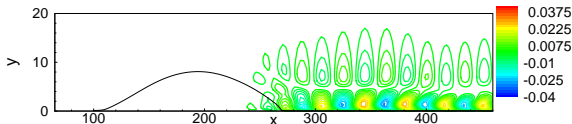
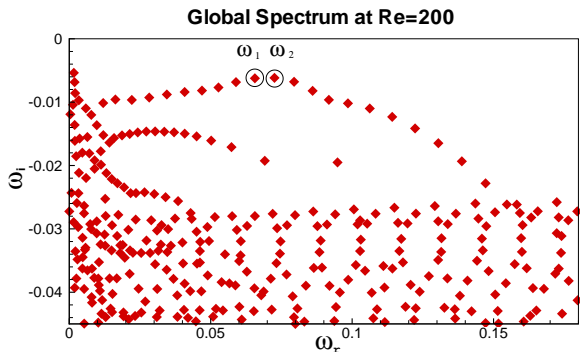
$Re = 225$



## Base flows at $150 < Re < 230$

- For subcritical Reynolds numbers, the base flow is computed by DNS.
- For supercritical Reynolds numbers, the base flow is computed by a continuation method combining the DNS approach with a Newton steady-state solver (Tuckerman & Barkley, 2000).

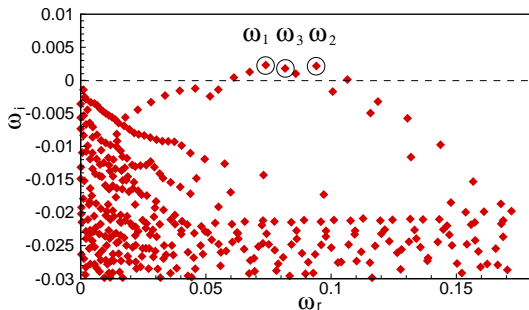
# Asymptotic subcritical dynamics



The spectrum is found to be stable. Three families of modes can be detected, two of them having a very low growth rate. The eigenvectors corresponding to the modes on the most unstable branch, are reminiscent of the classical TS modes predicted by a local approach.

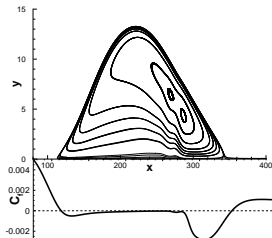
# Asymptotic supercritical dynamics

## Global spectrum at $Re=225$



The spectrum is unstable. Its structure is similar to the one at  $Re = 200$ , with 7 slightly unstable modes whose eigenvectors are reminiscent of the TS modes.

A marginal secondary separation begins to be recovered within the primary one at  $Re = 225$ , supporting the hypothesis of Dallmann et al. (1995) that topological changes in the base flow could be at the origin of the onset of unsteadiness in separation bubbles.



# Optimal energy gain

The maximum energy gain at time  $t$  over all possible initial conditions  $\mathbf{u}_0$  is defined as:

$$G(t) = \max_{\mathbf{u}_0 \neq 0} \frac{E(t)}{E(0)}. \quad (4)$$

where  $E(t) = \frac{1}{2} \int_0^{L_x} \int_0^{L_y} (\tilde{u}^2 + \tilde{v}^2) dx dy$

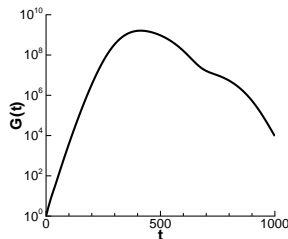
By decomposing the perturbation into the eigenmodes basis (2), it is possible to rewrite it as

$$G(t) = \|\mathbf{F} \exp(-it\mathbf{\Lambda})\mathbf{F}^{-1}\|_2^2 = \|\mathbf{\Gamma}\|$$

where  $\mathbf{\Lambda}_{k,l} = \delta_{k,l}\omega_k$  and  $\mathbf{F}$  is the Cholesky factor of the energy matrix  $\mathbf{M}$  of components

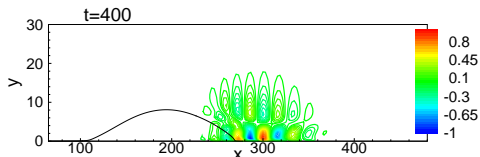
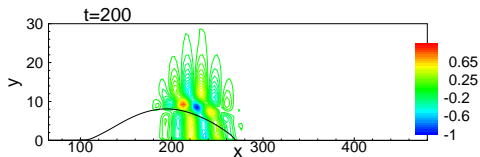
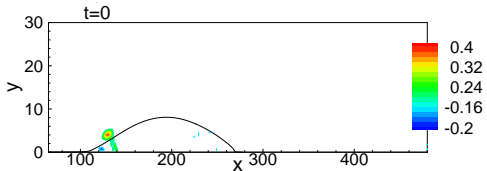
$$M_{ij} = \iint (\hat{u}_i^* \hat{u}_j + \hat{v}_i^* \hat{v}_j) dx dy, \quad i, j = 1, \dots, N$$

The maximum gain at time  $t$  and the corresponding  $\mathbf{u}_0$ , are computed by a singular value decomposition of  $\mathbf{\Gamma}$ .



Maximum energy gain  $G(t)$  computed with  $N = 600$  modes for  $Re = 200$ . The peak reaches a maximum of  $10^9$ , meaning that the flow has a high degree of non-normality.

# Optimal perturbation at $Re = 200$

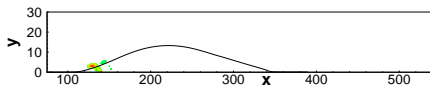


## Streamwise velocity contours of the optimal perturbation at $t = 0, 200, 400$

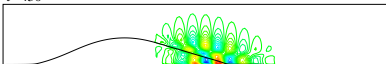
- 1 The initial energy is concentrated at the upstream part of the bubble.
- 2 The disturbance is convected downstream along the separation streamline amplifying itself until reaching the reattachment point.
- 3 The perturbation is convected through the attached boundary layer, where it is damped.

*The high amplification is due to the local convective KH instability of the velocity profiles within the bubble, leading to a global growth of perturbations.*

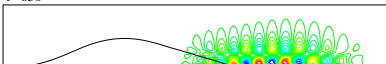
# Optimal perturbation at $Re = 225$



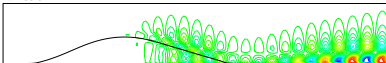
t=450



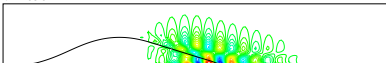
t=650



t=850



t=1050



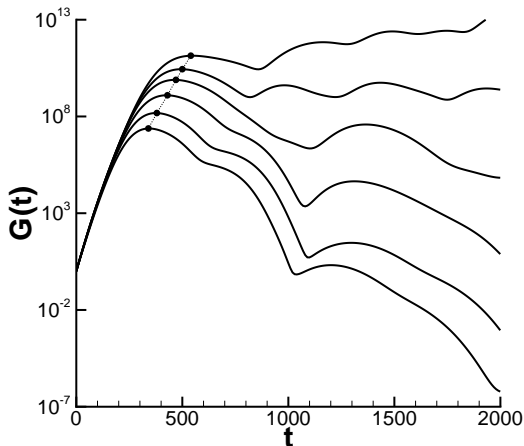
Streamwise velocity contours of the optimal perturbation at  $t = 0, 450, 650, 850, 1050$

- 1 The initial energy is concentrated at the upstream part of the bubble.
- 2 The disturbance is convected downstream by the mean flow as a localized wave packet.
- 3 A second wave packet is generated due to the amplification of the disturbances carried back by the recirculation bubble.

*A wave packet cycle is established asymptotically*

# Dependence of the optimal energy gain on $Re$

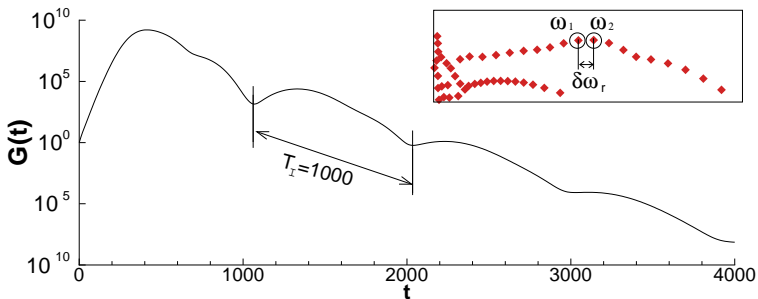
Optimal energy gain at  $Re = 190, 200, 207, 213, 219, 225$ .



- The first peak value and the time at which it occurs increase linearly with respect to  $Re$
- Such a linear increase could be due to the linear increase of the size of the bubble with  $Re$ , the global energy growth being due to the KH amplification at the separation streamline.

**At large times, modulations are recovered in the energy gain curves at all Reynolds numbers.**

# Flapping at subcritical Reynolds

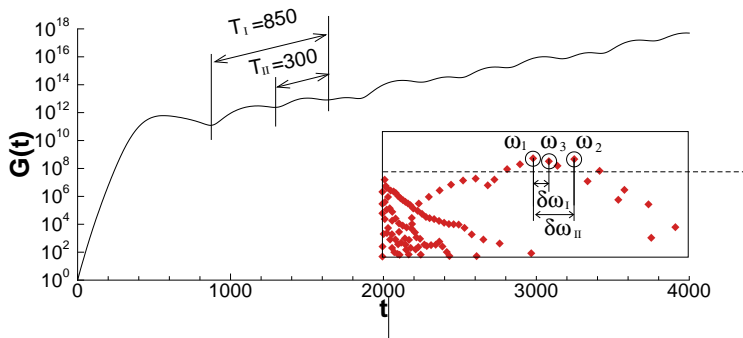


The most unstable modes,  $\omega_1$  and  $\omega_2$ , having comparable amplification rate and being associated to similar eigenvectors, interact resulting in a low-frequency modulation (**flapping**)

$$\delta\omega_r = 0.006 \rightarrow T = 2\pi/\delta\omega_r \approx 1000$$

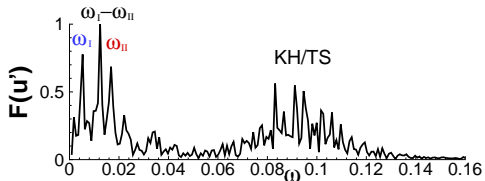
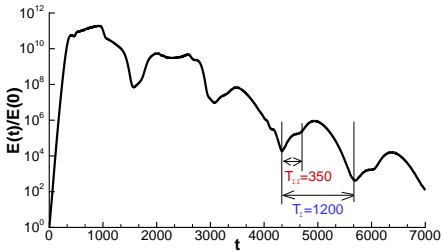
# Flapping at supercritical Reynolds

For  $Re \geq 213$ , **two low-frequencies** could be identified in the energy gain curve, due to the presence of three interacting unstable modes having very similar amplification rate and eigenvectors.



In Figure, at  $Re = 225$ ,  $\delta\omega_{rI} = \omega_{r3} - \omega_{r1} \approx 0.0075$ ,  $\delta\omega_{rII} = \omega_{r2} - \omega_{r3} \approx 0.02$  resulting in the periods  $T_I = 2\pi/\delta\omega_{rI} \approx 850$ ,  $T_{II} = 2\pi/\delta\omega_{rII} \approx 300$

# Recovering flapping by DNS at different Reynolds numbers

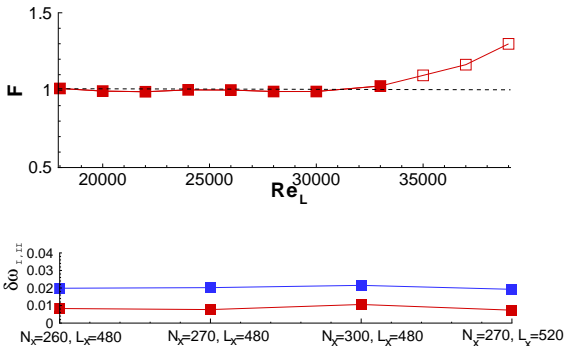


- At  $Re = 225$ , DNS recover a stable dynamics. Indeed, two modulations ( $T_I \approx 1200$  and  $T_{II} \approx 350$ ) affect the energy gain curve when a linear behaviour is established.
- At  $Re = 230$ , DNS recover an unstable dynamics. By a Fourier transform, the two flapping frequency ( $\omega_I \approx 0.006$ ,  $\omega_{II} \approx 0.0017$ ) as well as their difference are found. The higher frequencies correspond to the unstable global modes of the spectrum.

# Dependence of the flapping frequency with respect to $Re$

Is there any characteristic scale for the flapping frequency?

Let us consider a Reynolds number based on a fixed length  $L$ ,  $Re_L = U_\infty L / \nu$ , and the corresponding dimensionless frequency  $F = L / \delta^* f$ .



By the eigenvalue analysis, we find  $F \approx 1$  for any  $Re_L < 35000$  ( $Re < 213$ ), that is the threshold for the onset of the secondary flapping frequency.

→ *The values of the flapping frequencies are well converged with respect to grid resolution and domain length*

# Scaling law

Is there any physical explication for the flapping phenomenon?

**Hypothesis** : the separation, carrying back the perturbation in the upstream part of the bubble, could induce an interaction of modes producing the beating.

- A characteristic scale could be the time needed by the mean flow to carry back a wave packet from the reattachment to the separation point:

$$F \propto 1/t_L \propto U_b/L_b$$

$L_b$  being the bubble size and  $U_b$  the base flow velocity within the bubble.

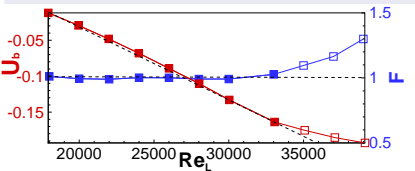
- $L_b$  and  $U_b$  vary linearly with respect to  $Re_L$  for  $Re_L < 35000$  ( $Re < 213$ )
- As long as  $Re_L < 35000$ ,

$$\frac{F_2}{F_1} = \frac{t_{L_1}}{t_{L_2}} = \frac{U_{b_2} L_{b_1}}{U_{b_1} L_{b_2}} = \frac{Re_{L_2} Re_{L_1}}{Re_{L_1} Re_{L_2}} = 1 \quad (5)$$

confirming that the flapping frequency  $F$  is constant with respect to  $Re$ .

# Role of topological changes in the flapping phenomenon (1)

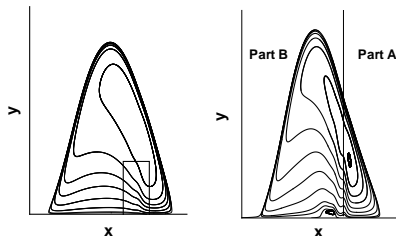
What happens at  $Re_L = 35000$ ?



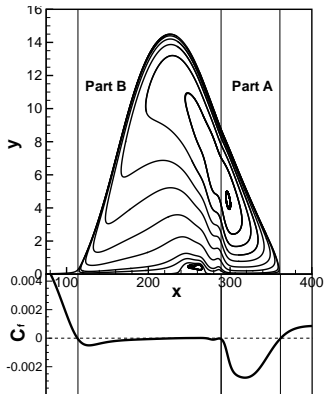
- The secondary flapping frequency appears
- The frequency  $F$  increases with  $Re$
- $U_b$  and  $L_b$  do not vary linearly with  $Re$
- Topological changes appear in the bubble

Could be these events linked?

***The inflection of the streamlines could lead the bubble to split in two smaller ones, A and B, which could carry back the perturbations at two different rates generating two distinct modulations.***



# Role of topological changes in the flapping phenomenon (2)



## How to validate the hypothesis of bubble splitting?

- The ratio of the size of bubble A with respect to the size of the bubble B ( $L_B/L_A \approx 2.5$ ) is close to the ratio of the two flapping frequencies ( $\omega_{II}/\omega_I \approx 2.7$ )
- For  $Re_L > 35000$  the primary beating is generated by the part B of the bubble, which is smaller than the entire bubble, and is able to carry back disturbances in a smaller time, originating a higher primary beating frequency.
- More validations need to be carried out, involving bubbles with different aspect ratio or geometry-induced-separations (generated by a bump or a backward-facing step).

# Conclusions

- The considered separated flow become unstable when a secondary bubble originate within the primary one, supporting the hypothesis of Dallmann et al (1995).
- For  $Re < 213$ , a **low-frequency beating** is found within the flow, whose value is constant with respect to  $Re$ .
- For  $Re \geq 213$ , when **topological changes** are recovered on the base flow, a secondary flapping frequency appears, while the primary one increases.
- A **scaling law** has been developed, based on the assumption that the oscillations are due to the interaction of the main wave packet with the perturbations carried upstream by the backflow, explaining the previous findings.
- Future works would aim at carry out more validations of such an hypothesis, for adverse-pressure as well as geometry-induced bubbles.